

Integrating machine learning and quantitative structure activity relationship (QSAR) modeling approaches to develop artificial intelligence (AI)-assisted interactive physiologically based pharmacokinetic (iPBPK) modeling web dashboard

---- SOT, RASS/BMSS/AACT Joint Webinar, December 13, 2023

Zhoumeng Lin, BMed, PhD, DABT, CPH, ERT

Center for Environmental and Human Toxicology (CEHT) & Center for Pharmacometrics and Systems Pharmacology (CPSP)
Department of Environmental and Global Health, College of Public Health and Health Professions (primary appointment)
Department of Physiological Sciences, College of Veterinary Medicine (jointly appointed)
Department of Pharmaceutics, College of Pharmacy (jointly appointed)
University of Florida, Gainesville, FL 32610

Outline

Introduction

- Research overview
- Background and terminology (PBPK, QSAR, ML, AI)

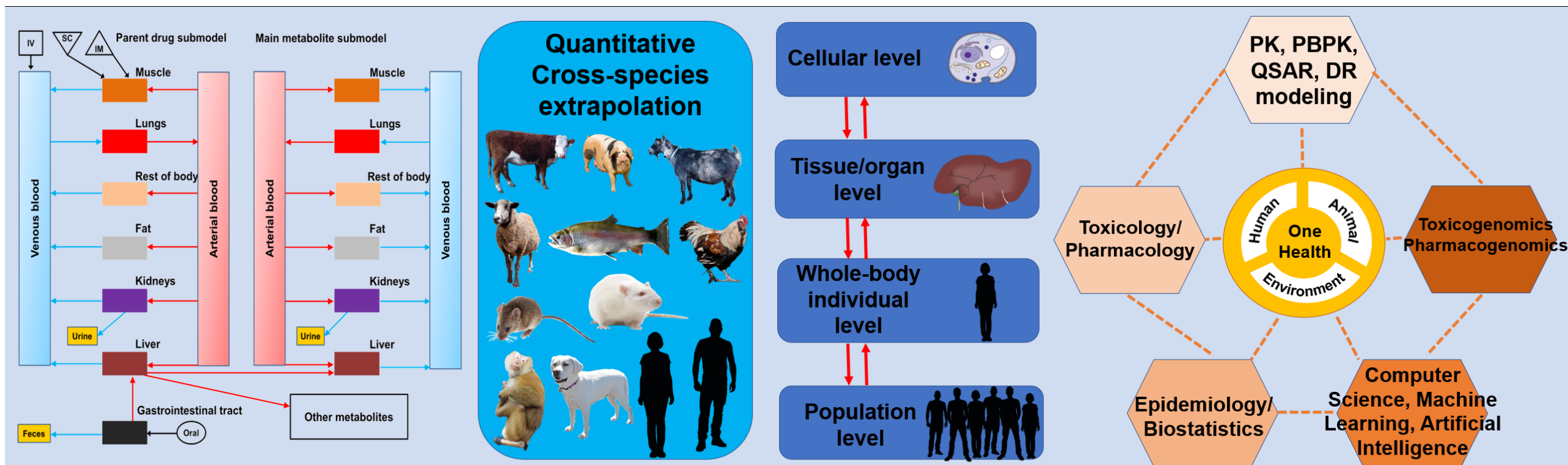
Different Applications

- AI in predicting ADME of chemicals
- AI in predicting toxicity of chemicals
- AI-assisted PBPK model for nanoparticles

Summary

- Summary and Discussion
- Acknowledgements

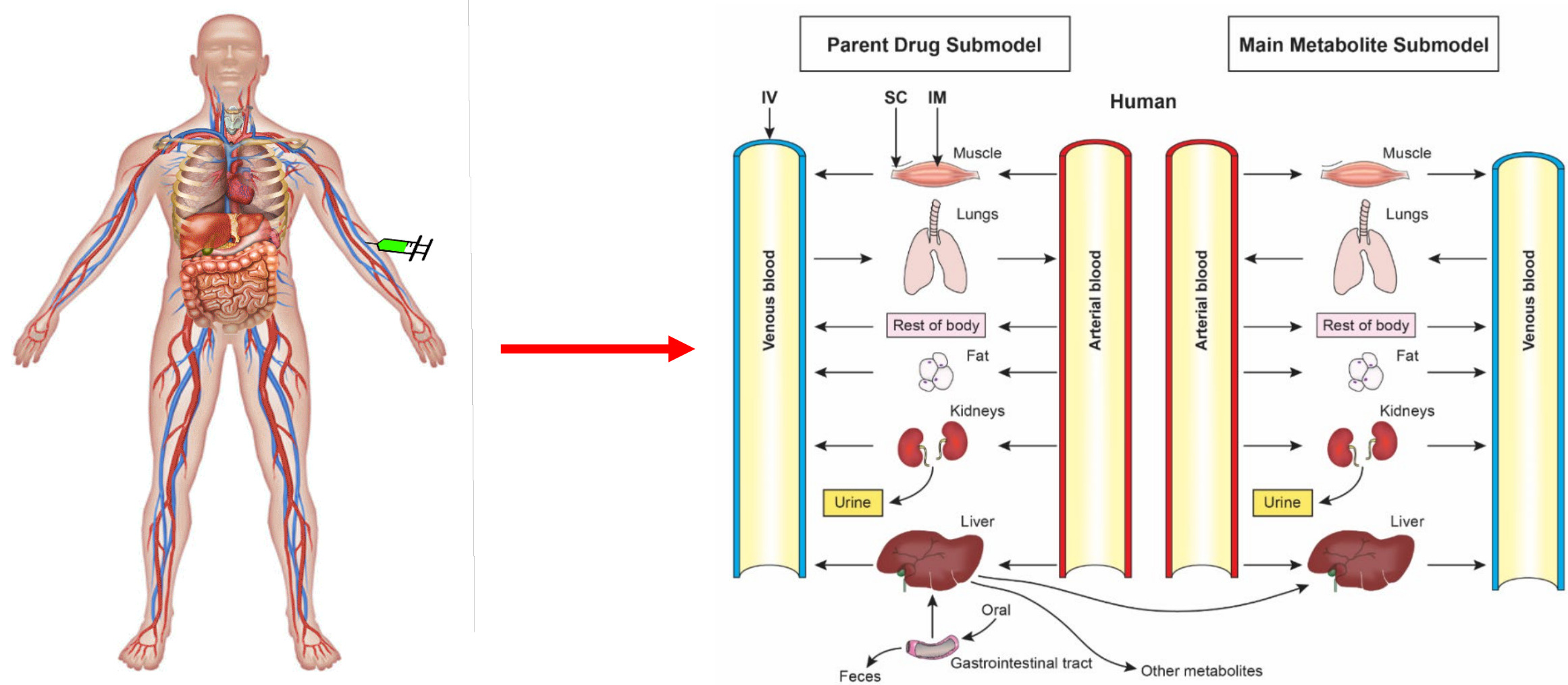
Research Program in Computational Toxicology and Pharmacology



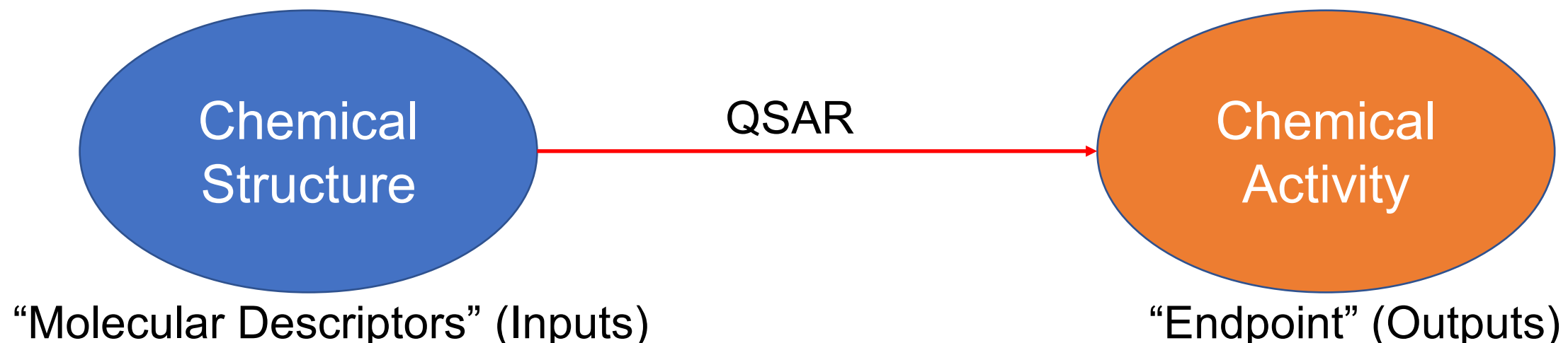
We develop computational models to address nanomedicine, animal-derived food safety, human health risk assessment issues!



What is Physiologically Based Pharmacokinetic (PBPK) Modeling?



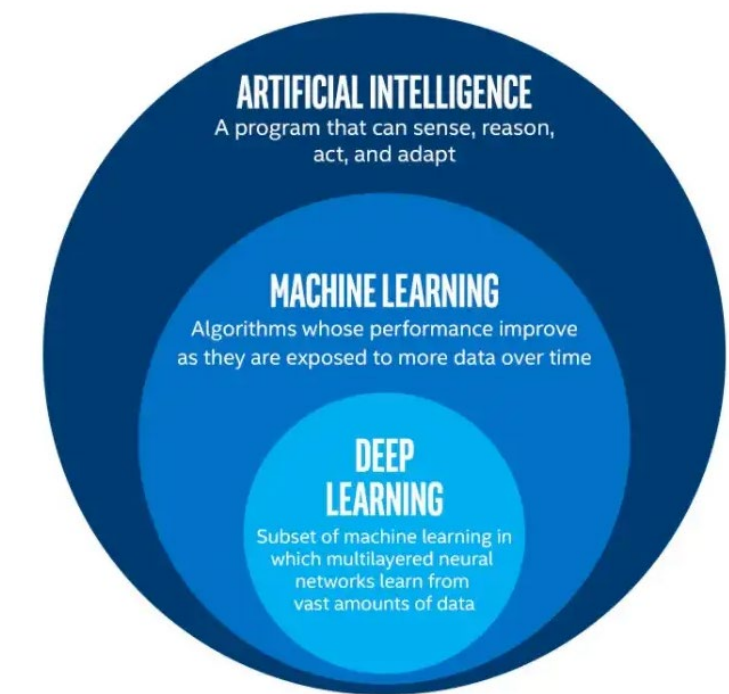
What is Quantitative Structure-Activity Relationship (QSAR) modeling?



- Quantitative structure activity relationship analysis (QSAR): the study of the relationship between chemical structure and biological properties of substances.
- These activities include absorption, distribution, metabolism, and excretion (ADME), as well as toxicity properties.

Machine Learning (ML) and Artificial Intelligence (AI)

- Artificial intelligence (AI) is a rapidly developing subdiscipline of computer science with the goal of designing and creating machines or computational models that can perform a variety of cognitive tasks at a level comparable or even exceed human intelligence.
- In this presentation, it mainly refers to the applications of various machine learning methods in the prediction and evaluation of chemical toxicokinetic (i.e., absorption, distribution, metabolism, and excretion [ADME]) and toxicity properties.
- Machine learning (ML) is a subarea of artificial intelligence, and it refers to mathematical or computer algorithms designed to teach or train a computational model to solve a problem or perform complex tasks based on some input parameters.



- Physiologically based pharmacokinetic (PBPK) modeling
- Quantitative structure-activity relationship (QSAR) modeling
- Adverse outcome pathway (AOP) analysis
- High-content image-based screening
- Toxicogenomics

CONTEMPORARY REVIEW

Machine Learning and Artificial Intelligence in Toxicological Sciences

Zhoumeng Lin *^{,†,1} and Wei-Chun Chou *^{,†}

*Department of Environmental and Global Health, College of Public Health and Health Professions, University of Florida, Gainesville, Florida 32610, USA; and [†]Center for Environmental and Human Toxicology, University of Florida, Gainesville, Florida 32608, USA

¹To whom correspondence should be addressed at Department of Environmental and Global Health, College of Public Health and Health Professions, University of Florida, 1225 Center Drive, Gainesville, FL 32610, USA. E-mail: linzhoumeng@ufl.edu.

Commonly Used Machine Learning Methods in Toxicology

Table 1. A List of Machine Learning Methods Commonly Used in Toxicological Research

Method	Brief Description
Supervised linear methods	
Multiple linear regression	Use multiple explanatory variables to predict the outcome of a response variable with a multivariate linear equation
Naïve Bayes classifier	Based on Bayes' theorem with strong assumptions of conditional independence among molecular descriptors (ie, explanatory variables)
Supervised nonlinear methods	
k-nearest neighbors	Classify a test chemical by looking for the training chemicals with the nearest distance to it
Support vector machine	Map molecular descriptor vectors into a higher dimensional feature space to build a maximal margin hyperplane to distinguish active (toxic) from inactive (nontoxic) chemicals
Decision trees	Each model is a series of rules organized in the format of a tree containing a single root node and any number of internal nodes and several leaf nodes. The path from the root to a leaf stands for a sequence of classification rules predicting a toxicity endpoint for a given chemical
Ensemble learning	Combine several base models into a more predictive one. Popular types of ensemble modeling include bagging, random spaces, boosting, and stacking.
Random forest	Combine the bagging with the random spaces approaches in application to decision trees base models
Artificial neural networks	
Backpropagation neural networks	All neurons are divided into 3 layers, with information flowing from the first layer of input neurons to the second layer of hidden neurons, and then to the third layer of output neurons
Bayesian-regularized neural networks	Apply Bayesian methods to perform regularization so that the model complexity is balanced against the accuracy of reproducing training data
Associative neural networks	Apply ensemble learning to backpropagation neural networks
Deep neural networks	Artificial neural networks with multiple hidden layers (also called deep learning)
Unsupervised methods	
Principle component analysis	Reduce the dimensionality of the data to only the first few principal components while preserving as much of the data's variation as possible
Kohonen's self-organizing maps	Map molecules from the original descriptor space onto a 2D grid of neurons. Similar molecules will be mapped to the same closely located neurons in the grid

This table is based on the book chapter by [Baskin \(2018\)](#). Please refer to [Baskin \(2018\)](#) for detailed description about each of the listed machine learning algorithms.

List of Studies using ML in QSAR Modeling to Predict Toxicity

Table 2. Representative Studies Integrating Machine Learning Approaches With Quantitative Structure-Activity Relationship Modeling

Best Machine learning Method	Training Dataset	Endpoint	Reference
Deep learning (ie, DeepTox)	11 764 chemicals from Tox21	12 bioassays	Mayr et al. (2016)
Ensemble extreme gradient boosting	1003 chemicals	Carcinogenicity	Zhang et al. (2017)
Random forest	Over 866 000 chemical properties/hazards	Acute oral and dermal toxicity, eye and skin irritation, mutagenicity, and skin sensitization	Luechtefeld et al. (2018)
Ensemble support vector machine	400 chemicals	Aquatic acute toxicity	Ai et al. (2019)
Multitask neural networks and graph convolutional networks	1012 PFAS	Bioactivity on 26 bioassays	Cheng and Ng (2019)
Extra trees	Over 1000 chemicals from different databases	Various toxicities	Pu et al. (2019)
Ensemble model	7385 chemicals	Acute toxicity in rats	Russo et al. (2019)
Support vector machine	482 chemicals	Acute toxicity in fathead minnow	Chen et al. (2020)
Deep learning (ie, CapsCarcino)	1003 chemicals from CPDB	Carcinogenicity	Wang et al. (2020)
Kernel-weighted local polynomial approach	Hundreds of chemicals depending on the species	Acute aquatic toxicity	Gajewicz-Skretna et al. (2021)
Meta ensembling of multitask deep learning models (ie, QuantitativeTox)	Hundreds to thousands of compounds depending on the endpoint	LD ₅₀ and LC ₅₀	Karim et al. (2021)
Deep learning-based model-level representations (ie, DeepCarc)	692 chemicals	Carcinogenicity	Li et al. (2021)
Extra trees	Over 18 600 drug-bacteria interactions	Gut bacterial growth	McCoubrey et al. (2021)
Support vector machine	676 pesticides	Acute contact toxicity on honey bees	Xu et al. (2021)
A consensus model based on 4 algorithms	1244 chemicals	Prenatal developmental toxicity	Ciallella et al. (2022)
Deep learning	31 chemicals with known or suspected clinical skin toxicity	Skin toxicity	Hu et al. (2022)
Random forest	1476 food contact chemicals	Carcinogenicity	Wang et al. (2022)

CPDB, Carcinogenic Potency Database. LC₅₀ and LD₅₀ refer to the compound concentrations that kill half the members of the tested animal population, respectively.

Studies That Used ML/AI to Predict ADME for Pharmaceutical Compounds

Table 2. A List of Representative Studies That Used Machine Learning and Artificial Intelligence Approaches in the Predictions of Absorption, Distribution, Metabolism, and Excretion Properties for Pharmaceutical Compounds

References	N	Predict Target	Descriptor Types	Modeling Method	Performance ^a
Absorption					
Agatonovic-Kustrin et al. (2001)	86	HIA	0D–3D theoretical descriptors	ANN, RBF, GNN	Training set: $R^2 = 0.82$; RMSE = 0.59 Test set: RMSE = 0.90
Deconinck et al. (2007)	67	HIA	1D–3D theoretical descriptors plus one of Abraham's solvation parameters	MARS	Whole data set: RMSE = 7.2%; Whole data set: $R^2 = 0.93$
Niwa (2003)	86	HIA	0D–1D theoretical descriptors	GRNN, PNN	Training set: RMSE = 6.5 Test set: RMSE = 22.8
Talevi et al. (2011)	120	HIA	0D–3D Dragon theoretical descriptors	MLR, ANN, SVM	Training set: $R^2 = 0.8$; RMSE = 0.18 Test set: $R^2 = 0.66$; RMSE = 0.21
Yan et al. (2008)	52	HIA	Adriana Code and Cerius2 0D–2D theoretical descriptors	GA, PLS, SVM	Training set: $R^2 = 0.66$; RMSE = 12.5 Test set: $R^2 = 0.77$; RMSE = 16
Shen et al. (2010)	1593	HIA	1D–2D theoretical descriptors	SVM	Training set: $Q = 98.5\%$ Test set: $Q = 99\%$
Kamiya et al. (2021b)	184	P_{app}	Chemical descriptors (not specific descriptions)	SVM, PLS, RBF	Whole data set: $R = 0.84$ –0.85
Ghafourian et al. (2012)	310	HIA	A total of 215 descriptors (not specific descriptions)	MLR	Training set: RMSE = 14.54 Test set: RMSE = 23.84
Hou et al. (2007)	648	HIA	0D–2D theoretical descriptors	MARS, GA	Training set: $R^2 = 0.97$.3 Test set: $R^2 = 0.98$
Wang et al. (2017)	970	HIA	2D–3D descriptors, molecular fingerprints, and structural fragments	RF	Training set: SE = 0.89; SP = 0.85; $Q = 0.89$ Test set: SE = 0.88; SP = 0.81; $Q = 0.87$
Distribution					
Antontsev et al. (2021)	21	Kp	Not explained in the study	BIOiSIM	Test set: AFE = 0.96 (C_{max}), 0.89 (AUC), 0.69 (Vd); AAFFE = 1.2 (C_{max}), 1.30 (AUC), 1.71 (Vd); $R^2 = 0.99$ (C_{max}), 0.98 (AUC), 0.99 (Vd)
Golmohammadi et al. (2012)	310	Kp	3D descriptors and molecular structural information	SVM; GA, PLS	Training set: $R^2 = 0.98$, RMSE = 0.117 Test set: $R^2 = 0.98$, RMSE = 0.118
Liu et al. (2005)	208	Kp	Constitutional, topological, geometrical, electrostatic and quantum chemical descriptors	SVM	Training set: $R^2 = 0.97$, RMSE = 0.02 Test set: $R^2 = 0.974$, RMSE = 0.0289
Yun et al. (2014)	122	Kp	LogP, pKa, fu	DT; RF	Whole data set: $Q = 72\%$



SOT | Society of
Toxicology
academic.oup.com/toxsci

Toxicological Sciences, 2023, 191(1), 1–14
<https://doi.org/10.1093/toxsci/kfac101>
Advance Access Publication Date: 26 September 2022
Contemporary Review

Machine learning and artificial intelligence in physiologically based pharmacokinetic modeling

Wei-Chun Chou ^{1,2}, Zhoumeng Lin ^{1,2,*}

¹Department of Environmental and Global Health, College of Public Health and Health Professions, University of Florida, Gainesville, FL 32610, USA

²Center for Environmental and Human Toxicology, University of Florida, Gainesville, FL 32608, USA

*To whom correspondence should be addressed at Department of Environmental and Global Health, College of Public Health and Health Professions, University of Florida, 1225 Center Drive, Gainesville, FL 32610, USA. E-mail: linzhoumeng@ufl.edu.

Studies That Used ML/AI to Predict ADME for Pharmaceutical Compounds

Table 2.. (continued)

References	N	Predict Target	Descriptor Types	Modeling Method	Performance ^a
Metabolic					
Athersuch et al. (2013)	15		Classify the metabolic pathways of test compounds	PCA, PLS	Whole data set: $R^2 = 0.96$, $Q = 77.5\%$
Baranwal et al. (2020)	6669		Classify the metabolic pathways of test compounds	RF and GCN	Test set: $Q = 98.99\%$
Jia et al. (2020)	5682		Classify the metabolic pathways of test compounds	RF	Whole data set: $Q = 94\%$
Zhang et al. (2008)	44	V_{max} , K_m	Molecular fingerprints	ANN	Whole data set: $R^2 = 0.6\text{--}0.9$ (K_m), $R^2 = 0.6\text{--}0.7$ (V_{max}), RMSE = 0.3–0.5 (K_m), RMSE = 0.4–0.7 (V_{max})
Sarigiannis et al. (2017)	54	V_{max} , K_m	Physicochemical properties based on Abraham's solvation equation	ANN, NLR	Test set: $R^2 = 0.82$ (K_m), $R^2 = 0.99$ (V_{max})
Elimination					
Hsiao et al. (2013)	244	Cl_{int}	Molecular fingerprints, physico-chemical properties, and 3D quantum chemical descriptors	PLS, RF, PCA	Whole data set: $R^2 = 0.96$; $Q = 48\%$
Iwata et al. (2021)	748	Cl_{total}	The chemical structure was represented as graph data	DL	Test data set: GMFE = 2.68
Kosugi and Hosea (2020)	1114	Cl_{total}	2D SMARTS-based descriptors	RF, RBF	Whole data set: $R^2 = 0.55$, RMSE = 0.332
Paine et al. (2010)	349	Cl_{renal}	195 descriptors	RF	Training set: $R^2 = 0.93$, RMSE = 0.32 Test set: $R^2 = 0.63$, RMSE = 0.63
Paixao et al. (2010)	112	Cl_{int}	233 molecular descriptors	ANN	Training set: $R^2 = 0.953$, RMSE = 0.236 Test set: $R^2 = 0.804$, RMSE = 0.544
Wang et al. (2019)	1352	Cl_{total}	2D and 3D descriptors, and 49 fingerprints.	SVM, GBM, XGBoost	Training set: $R^2 = 0.882$, RMSE = 0.239 Test set: $R^2 = 0.875$, RMSE = 0.103
Gombar and Hall (2013)	525	Cl_{tot}	89 descriptors calculated from electro-topological state (E-state) fingerprints	SVM, MLR	Test set: $R^2 = 0.70$

Abbreviations: AAFE, absolute average fold error; AFE, absolute fold error; ANN, artificial neural networks; Cl_{int} , intrinsic metabolic clearance; Cl_{renal} , renal clearance; Cl_{total} , total plasma clearance; DL, deep learning; DT, decision tree; GA, generic algorithm; GBM, gradient boosting machine; GCN, graphical conventional network; GMFE, geometric mean fold error; GNN, general neural network; GRNN, general regression neural network; F, oral bioavailability; HIA, human intestinal absorption; K_m , Michaelis constant; MARS, multivariate adaptive regression splines; MLR, multiple linear regression; NLR, nonlinear regression; Papp, apparent membrane permeability coefficients; PCA, principle component analysis; PLS, partial least squares; PNN, probabilistic neural network; Q, prediction accuracy; R^2 , squared Pearson's correlation coefficient; RBF, radial basis function; RF, random forest; RMSE, root-mean-square error; SVM, support vector machine; V_{max} , maximal reaction rate; XGBoost, eXtreme Gradient Boosting.

^aThe performance from the best model.

Studies That Used ML/AI to Predict ADME for Nonpharmaceutical Compounds

Table 3. A List of Representative Studies That Used Machine Learning and Artificial Intelligence Approaches in the Predictions of Toxicokinetic Parameters for Nonpharmaceutical Compounds

References	N	Predict Target	Descriptor Types	Modeling Method	Performance ^a
Wambaugh et al. (2015)	271	Transporter affinity	NA	RF	NA
Ingle et al. (2016)	1651	Fub	2D molecular descriptors	kNN, SVM, RF	Training set: $R^2 = 0.82$, RMSE = 0.59 Test set: $R^2 = 0.51$; RMSE = 0.218
Watanabe et al. (2018)	2738	Fub	2D molecular descriptors	kNN, SVM, RF, PLS	Test set: $R^2 = 0.728$; RMSE = 0.145
Papa et al. (2018)	1000	Cl_{int}	2-3D molecular descriptors	PLS	Whole data set: $R^2 = 0.80$, RMSE = 0.62
Pradeep et al. (2020)	1487	Fub, Cl_{int}	0-3D molecular descriptors	SVM, RF, ANN	Fub: Training set: $R^2 = 0.56$, RMSE = 0.82; Test set: $R^2 = 0.57$, RMSE = 0.80 Cl_{int} : Training set: $R^2 = -0.00$, RMSE = 0.46; Test set: $R^2 = 0.16$, RMSE = 0.40
Dawson et al. (2021)	6484	Fub, Cl_{int}	1-3D molecular descriptors	RF	Fub: Training set: $R^2 = 0.584$, RMSE = 0.206; Test set: $R^2 = 0.591$, RMSE = 0.187 (Environment chemicals from ToxCast) Cl_{int} : Test set: Q = 0.55 (Class 1), 0.12 (Class 2), 0.90 (Class 3)
Yun et al. (2021)	818	Fub	2D molecular descriptors	kNN, SVM, RF, PLS	Test set: $R^2 = 0.52$, Mean absolute error = 12.6

Abbreviations: ANN, artificial neural networks; Cl_{int} , intrinsic metabolic clearance; PLS, partial least squares; PNN, probabilistic neural network; Q, prediction accuracy; R^2 , squared Pearson's correlation coefficient; RF, random forest; RMSE, root mean square error; SVM, support vector machine.

^aThe performance from the best model.

A List of Databases That Contains PK Data for Machine Learning Analysis

Table 1. A list of databases that contain pharmacokinetic data for machine learning analyses

Database name	Number of compounds	PK parameters	Description	Website	References
PK-DB	676	Cl, $t_{1/2}$, AUC, C_{max} , Kel and PK time-courses data	PK-DB is a comprehensive database, which contains data from human clinical trials and provides curated PK information on characteristics of studied patient cohorts, applied interventions, PK parameters, and PK time-courses data.	https://pk-db.com	Grzegorzewski et al. (2021)
PK/DB	1203	HIA, F, fu, BBB, Vd, Cl, $t_{1/2}$	PK/DB is a robust database for PK studies and in silico ADME prediction.	www.pkdb.ifsc.usp.br	Moda et al. (2008)
PKKB	1685	HIA, fu, Vd, Cl, LD50	Pharmacokinetic Knowledge Base (PKKB) is a comprehensive database of PK and toxic properties for drugs.	http://cadd.suda.edu.cn/admet	Cao et al. (2012)
e-Drug3D	1852	Vd, Cl, $t_{1/2}$, PPB, F, C_{max} , and Tmax	e-Drug3D is a database of 1852 FDA-approved drugs with 3-D chemical structures and information on PK parameters	https://chemoinfo.ipmc.cnrs.fr/MOLDB/index.php	Pihan et al. (2012)
ChEMBL	>1M	Not available	Open-access database containing ADME and toxic information for numerous drug-like compounds	www.ebi.ac.uk/chembl/	Gaulton et al. (2012)
Lombardo's database	1352	Vd, Cl, MRT, fu, $t_{1/2}$	A human intravenous PK data set derived from the literature.	Not available	Lombardo et al. (2018)
Wang's database	970	HIA	A human intestinal absorption data set consists of 970 compounds, and 9 different types of descriptors.	Not available	Wang et al. (2017)
CvT	144	PK time-course data	A public database of chemical time-series concentration data for 144 environmentally relevant chemicals and their metabolites	https://github.com/USEPA/CompTox-PK-CvTdb	Sayre et al. (2020)

Abbreviations: AUC, area under curve; BBB, blood brain barrier; Cl, clearance; Cmax, maximum concentration; F, oral bioavailability; fu, fraction unbound in plasma; HIA, human intestinal absorption; Kel, elimination rate; LD, lethal dose; MRT, mean residence time; PK, pharmacokinetic; PPB, plasma protein binding; $t_{1/2}$, terminal half-life; Tmax, time to peak drug concentration; Vd, volume of distribution.

A List of Databases Relevant to Computational Toxicology

Table 3. A List of Databases Relevant to Computational Toxicology

Database	Data Size ^a	Data Type	Reference
ACToR	Over 800 000 compounds and 500 000 assays	In vitro and in vivo toxicity	Judson et al. (2008)
Biosolids list	726 chemical pollutants	Concentration data in biosolids	Richman et al. (2022)
CEBS	Over 11 000 compounds and 8000 studies	Gene expression data	Lea et al. (2017)
ChEMBL	1.1 million bioassays, 1.8 million compounds, over 15 million activities	Literature data on binding, function, and toxicity of drugs and drug-like chemicals	Gaulton et al. (2012)
Connectivity map	Around 1300 compounds and 7000 genes	Gene expression data	Subramanian et al. (2017)
CTD	Over 14 000 compounds, 42 000 genes, 6000 diseases	Relationships among compounds, genes, and diseases	Davis et al. (2021)
DrugMatrix	Around 600 drug molecules and 10 000 genes	Gene expression data	Ganter et al. (2005)
GEO	Over 4300 subdata sets	Microarray, next-generation sequencing, and other forms of high-throughput functional genomics data	Barrett et al. (2013)
eNanoMapper	Over 700 types of nanomaterials	Diverse data types on nanomaterial physicochemical properties and safety	Jeliazkova et al. (2015)
MoleculeNet	Over 700 000 compounds	Quantum mechanics, physical chemistry, biophysics, and physiology	Wu et al. (2018)
Open TG-GATEs	170 compounds	Gene expression data and metadata	Igarashi et al. (2015)
PubChem	Over 111 million compounds, 1.39 million bioassays, and 293 million bioactivity data points	Toxicology, genomics, pharmacology, and literature data	Kim et al. (2021)
Pubvinas	11 types of nanomaterials with 705 unique nanomaterials	Up to 6 physicochemical properties and/or bioactivities	Yan et al. (2020)
REACH	21,405 unique substances with information from 89,905 dossiers	Data submitted in European Union chemical legislation	Luechtefeld et al. (2016)
RepDose	364 compounds investigated in 1017 studies, resulting in 6,002 specific effects	Repeat-dose study data in dogs, mice, and rats	Bitsch et al. (2006)
SEURAT	Over 5500 cosmetic-type compounds in the current COSMOS database web portal	Animal toxicity data	Vinken et al. (2012)
ToxicoDB	231 chemicals	Toxicogenomic data	Nair et al. (2020)
ToxNET	Over 50 000 environmental chemicals from 16 resources	In vitro and in vivo toxicity data	Fonger et al. (2000)

^a On the basis of live web counts or most recent literature publications as of March 2022. ACToR, Aggregated Computational Toxicology Resource; CTD, Comparative Toxicogenomics Database; CEBS, Chemical Effects in Biological Systems; GEO, Gene Expression Omnibus; Open TG-GATEs, a large-scale toxicogenomic database; REACH, Registration, Evaluation, Authorization, and Restriction of Chemicals; SEURAT, Safety Evaluation Ultimately Replacing Animal Testing; ToxNET, Toxicology Data Network. This table was adapted from Ciallella and Zhu (2019) with permission from the publisher.

Application 1: AI in Predicting ADME Properties

Application 1: AI-based PBPK/QSAR in predicting ADME of chemicals

Background



~94.4 million



~72.9 million



~5.23 million



~2.62 million



~8.54 billion



~238 million

Terminology

The meat withdrawal period or milk discard time is the interval between the time of the last administration of a new animal drug and the time when the animal can be safely slaughtered for food or the milk can be safely consumed.

The tolerance (or maximum residue limit [MRL]) is the maximum concentration of a marker residue, or other residue indicated for monitoring, that can legally remain in a specific edible tissue of a treated animal.

Extralabel drug use (ELDU) describes the use of an approved drug in a manner that is not in accordance with the approved labeling, yet meets the conditions set forth by the Animal Medicinal Drug Use Clarification Act of 1994 (AMDUCA) and U.S. Food and Drug Administration (FDA) regulations.

We use the term “**withdrawal interval**” when a drug is used extralabel.

The challenge in this field is how to calculate withdrawal interval after extralabel drug use.

Application 1: AI-based PBPK/QSAR in predicting ADME of chemicals

Food Animal Residue Avoidance Databank

(A component of the Food Animal Residue Avoidance & Depletion Program)

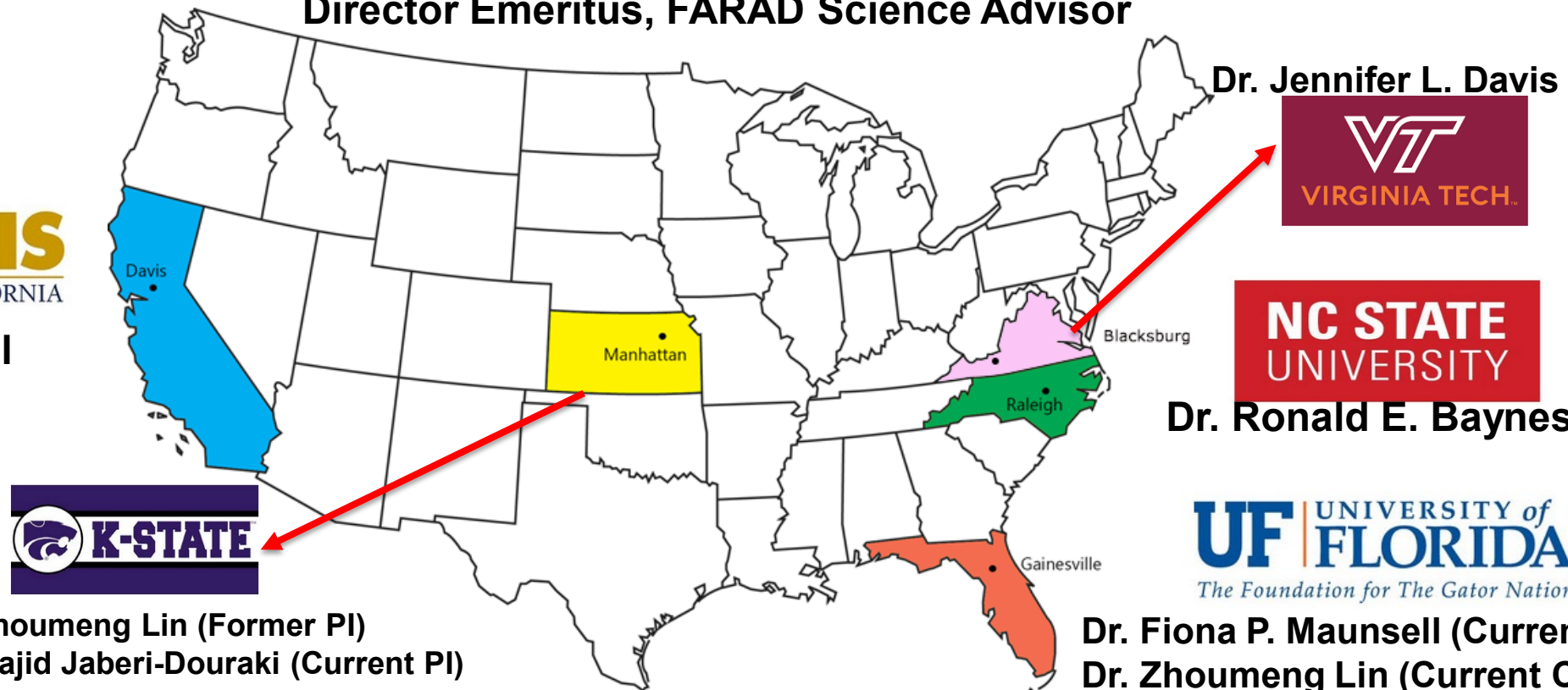


HOME PAGE ABOUT FARAD SERVICES RESOURCES REGULATORY INFO CONTACT FARAD IN THE NEWS

Google Custom Search

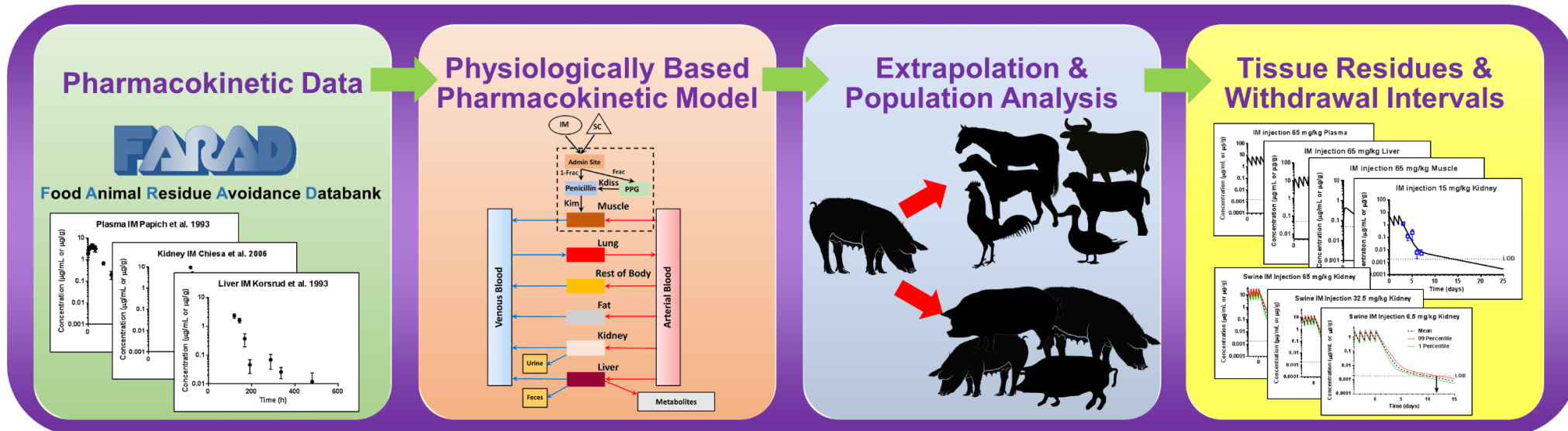
FARAD's primary mission is to help producers and veterinarians prevent or mitigate illegal or harmful residues of drugs, pesticides, biotoxins and other chemical agents that may contaminate foods of animal origin.

**Dr. Jim E. Riviere, Co-Founder,
Director Emeritus, FARAD Science Advisor**



Application 1: AI-based PBPK/QSAR in predicting ADME of chemicals

PK/PBPK Component of FARAD at UF



Objective: To develop web-based computational models/platforms that allow FARAD responders to easily calculate withdrawal intervals for drugs or other chemicals in different food animal species

Specific responsibilities:

- Develop PBPK and AI-QSAR models and web-based interfaces
- Provide pharmacokinetic and toxicokinetic support to other regional centers
- Provide advice on withdrawal intervals and potential food safety risk
- Provide training to FARAD responders on how to calculate withdrawal intervals

Application 1: Overview and timeline of our PK/PBPK models (KSU + UF)

2014-2016

- Established methodology
- Created PBPK models for drugs in an average animal
- Ceftiofur, enrofloxacin, flunixin, sulfamethazine
- Swine and Cattle

Lin et al. 2015. J Pharm Sci
 Lin et al. 2016. Sci Rep
 Lin et al. 2016. J Vet Pharmacol Ther

2016-2018

- Improved the methodology
- Monte Carlo simulation
- Created PBPK models for drugs in a diverse population of animals
- Penicillin G
- Swine, beef cattle, dairy cows

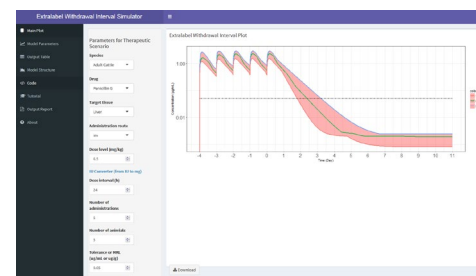
Lin et al. 2017. Toxicol Sci
 Li et al. 2017. Food Chem Toxicol
 Li et al. 2018. Toxicol Sci

2018-2023

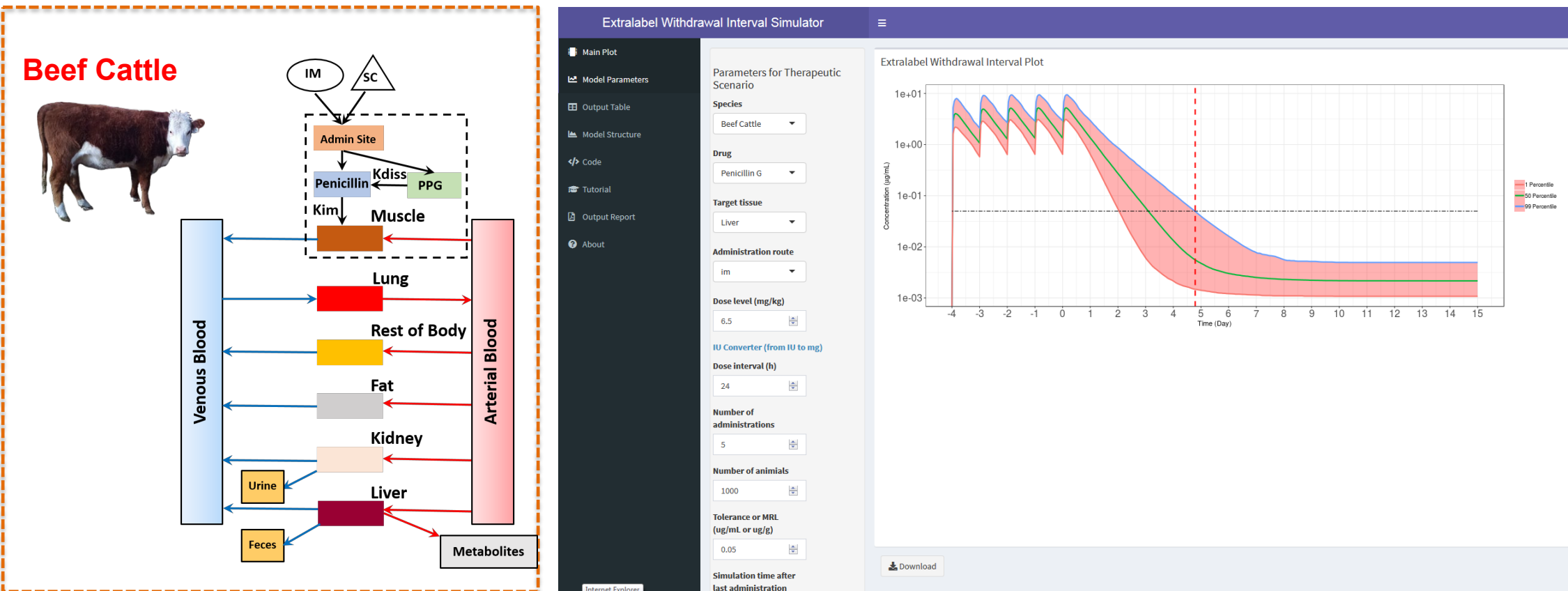
- Graphical user interface (GUI)
- Population PBPK models
- Penicillin G, flunixin, florfenicol, oxytetracycline, PFAS
- Physiological parameter database: cattle, swine, chickens, turkeys, sheep, goats
- Other quantitative methods from FDA & EMA

Li et al. 2019. Arch Toxicol
 Li et al. 2019. J Vet Pharmacol Ther
 Bates et al. 2020. BMC Vet Res
 Wang et al. 2021. J Vet Pharmacol Ther
 Lin et al. 2019. J Anim Sci
 Lin et al. 2020. J Vet Pharmacol Ther
 Smith et al. 2020. Front Vet Sci

Li et al. 2021. J Vet Pharmacol Ther
 Riad et al. 2021. Toxicol Sci
 Chou et al. 2022. Toxicol Sci
 Yuan et al. 2022. Food Chem Toxicol
 Yuan et al. 2022. Regul Tox Pharmacol
 Chou et al. 2023. Food Chem Toxicol
 Wu et al. 2023. Food Chem Toxicol



Application 1: Penicillin G PBPK model in cattle and swine



Li M, Gehring R, Riviere JE, Lin Z*. (2017). Development and application of a population physiologically based pharmacokinetic model for penicillin G in swine and cattle for food safety assessment. *Food and Chemical Toxicology*, 107:74-87.

Li M, Gehring R, Riviere JE, Lin Z*. (2018). Probabilistic physiologically based pharmacokinetic model for penicillin G in milk from dairy cows following intramammary or intramuscular administrations. *Toxicological Sciences*, 164(1):85-100.

Li M, Cheng YH, Chittenden JT, Baynes RE, Tell LA, Davis JL, Vickroy TW, Riviere JE, Lin Z*. (2019). Integration of Food Animal Residue Avoidance Databank (FARAD) empirical methods for drug withdrawal interval determination with a mechanistic population-based interactive physiologically-based pharmacokinetic (iPBPK) modeling platform: example for flunixin meglumine administration. *Archives of Toxicology*, 93(7):1865-1880. **(Best Postdoctoral Publication Award, 2020 Society of Toxicology)**

Halleran JL, Papich MG, Li M, Lin Z, Davis JL, Maunsell FP, Riviere JE, Baynes RE, Foster DM*. (2022). Update on withdrawal intervals following extralabel use of procaine penicillin G in cattle and swine. *Journal of the American Veterinary Medical Association*, 260(1): 1-6.

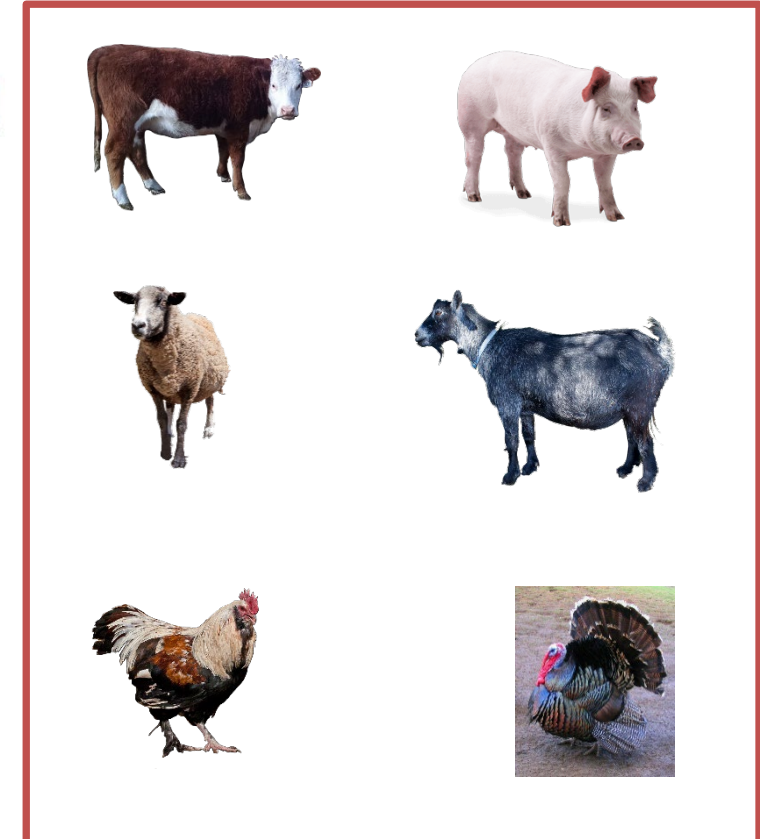
Application 1: Physiological parameters for PBPK modeling in food animals

Available at FARAD website (<http://farad.org/>), click Resources, and then click “PBPK Physiological Parameters”

FARAD Food Animal Residue Avoidance Databank 1-888-US-FARAD • 1-888-873-2723

Physiological Parameters for PBPK Modeling in Food Animals

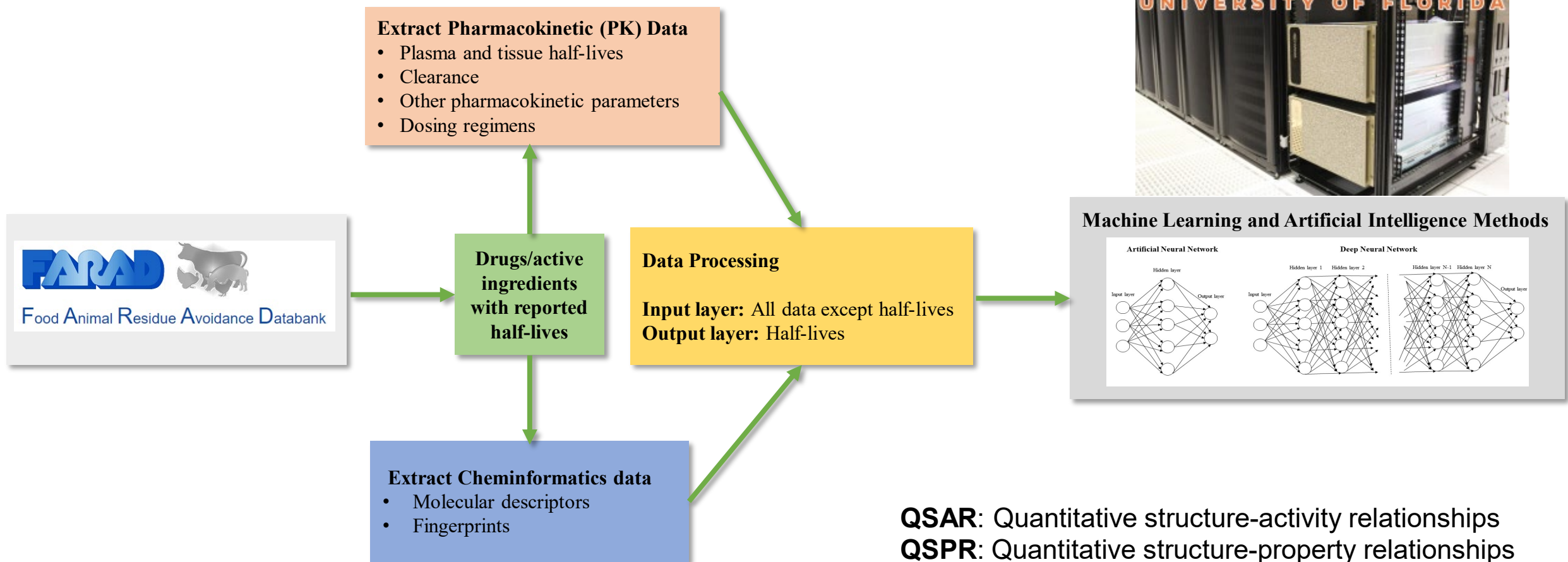
Animal	Parameter
<input type="radio"/> Adult Cattle <input type="radio"/> Market-Age <input type="radio"/> Calves <input type="radio"/> Growing <input type="radio"/> Beef Cattle <input type="radio"/> Aged <input type="radio"/> Male <input type="radio"/> Female <input type="radio"/> Angus <input type="radio"/> Different Age Groups <input type="radio"/> Chicken <input type="radio"/> Broiler <input type="radio"/> Laying Hens <input type="radio"/> Dairy Cows <input type="radio"/> Turkey <input type="radio"/> Sheep <input type="radio"/> Market-Age <input type="radio"/> Jersey <input type="radio"/> Holstein <input type="radio"/> Swine <input type="radio"/> Lambs <input type="radio"/> Goats	<input type="radio"/> Organ Weight <input type="radio"/> Cardiac Output <input type="radio"/> Blood Flow <input type="radio"/> Vascular Space Fraction <input type="radio"/> Hematocrit



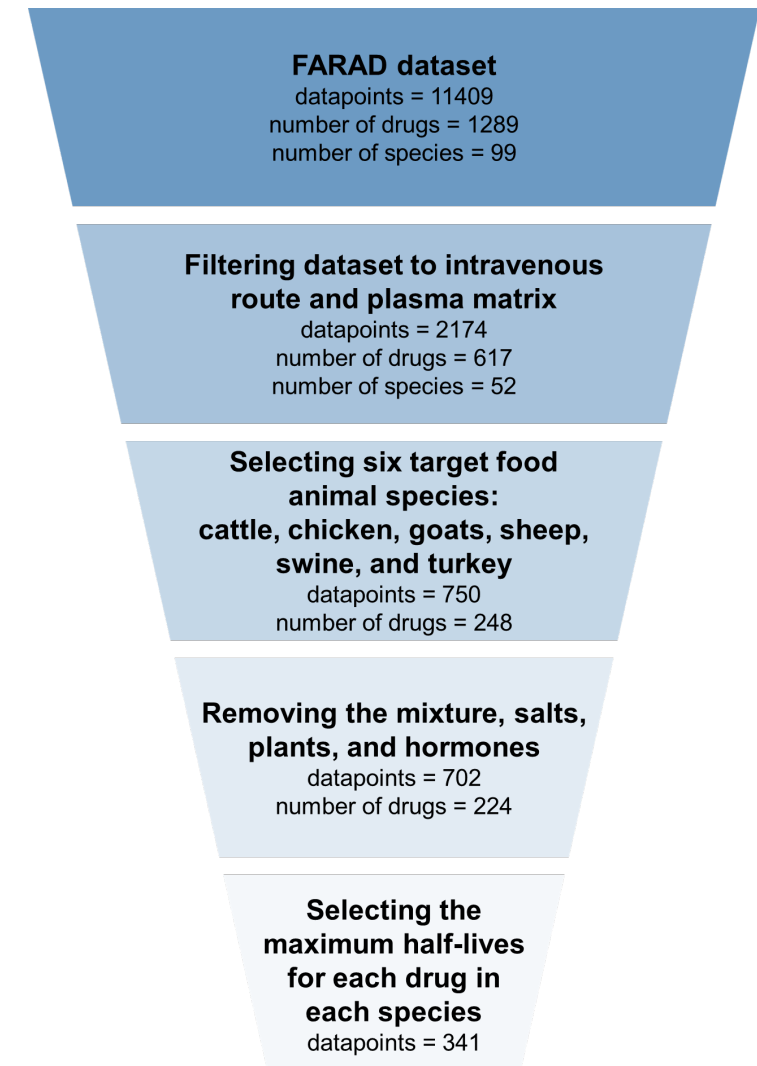
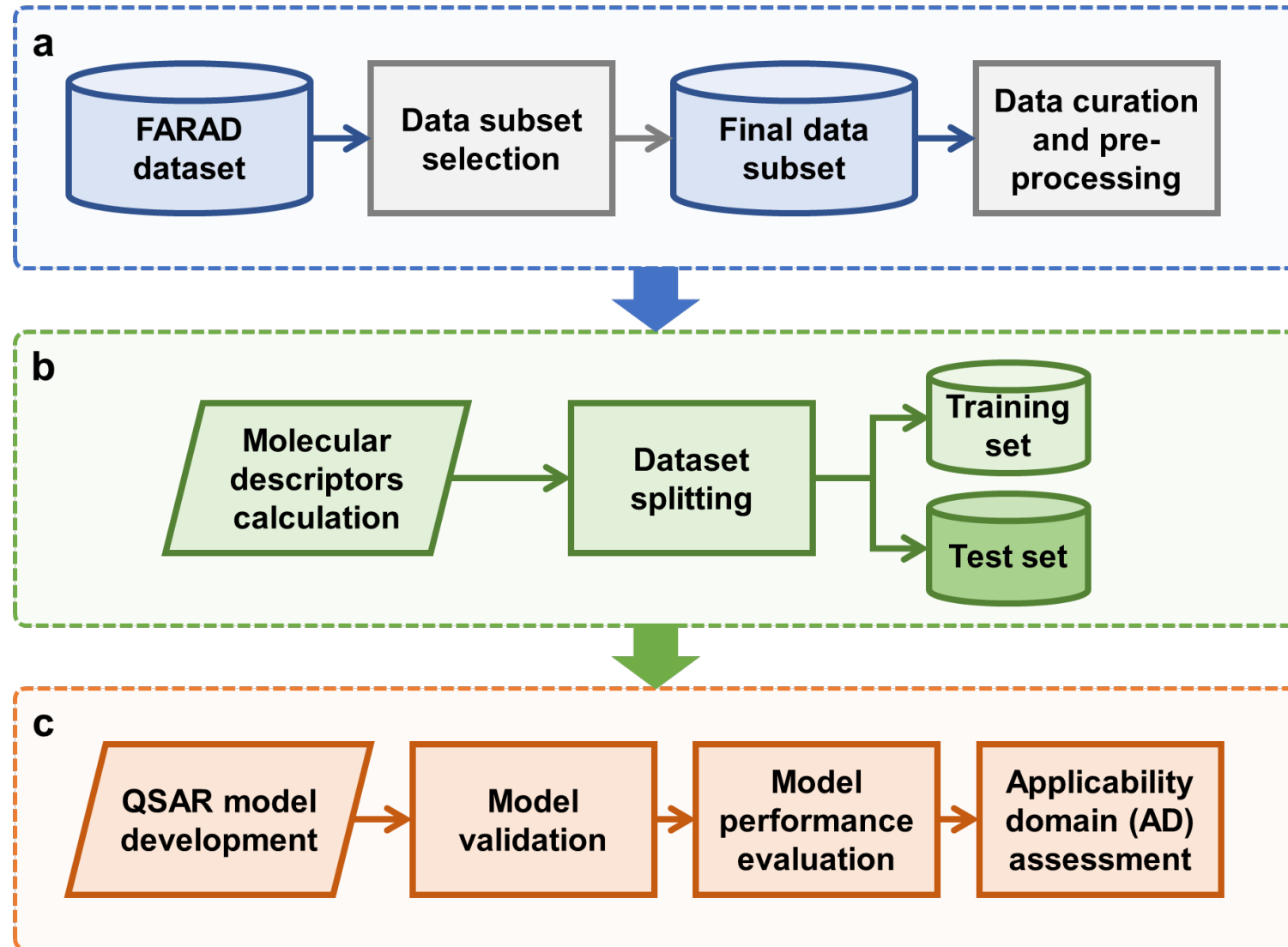
- Li M, Wang YS, Elwell-Cuddy T, Baynes RE, Tell LA, Davis JL, Maunsell FP, Riviere JE, Lin Z. (2021). Physiological parameter values for physiologically based pharmacokinetic models in food-producing animals. Part III: Sheep and goat. *Journal of Veterinary Pharmacology and Therapeutics*, 44(4), 456-477. **[Top Cited Article in this journal in 2022]**
- Wang YS, Li M, Tell LA, Baynes RE, Davis JL, Vickroy TW, Riviere JE, Lin Z. (2021). Physiological parameter values for physiologically based pharmacokinetic models in food-producing animals. Part II: Chicken and turkey. *Journal of Veterinary Pharmacology and Therapeutics*, 44(4), 423-455. **[Top Cited Article in this journal in 2022]**
- Lin Z, Li M, Wang YS, Tell LA, Baynes RE, Davis JL, Vickroy TW, Riviere JE. (2020). Physiological parameter values for physiologically based pharmacokinetic models in food-producing animals. Part I: Cattle and Swine. *Journal of Veterinary Pharmacology and Therapeutics*, 43(5):385-420. **[One of the Top 10 Most-Downloaded Articles of 2020 in this journal]**

Application 1: Role of AI and PBPK in animal-derived food safety assessment

- Long-term: Integration of AI with PBPK and/or QSAR/QSPR to predict PK properties of drugs
- Short-term: Build an AI-QSAR model to predict plasma half-life of animal drugs



Application 1: Schematic workflow of the AI-based QSAR model



Application 1: Preliminary results of the AI-QSAR model

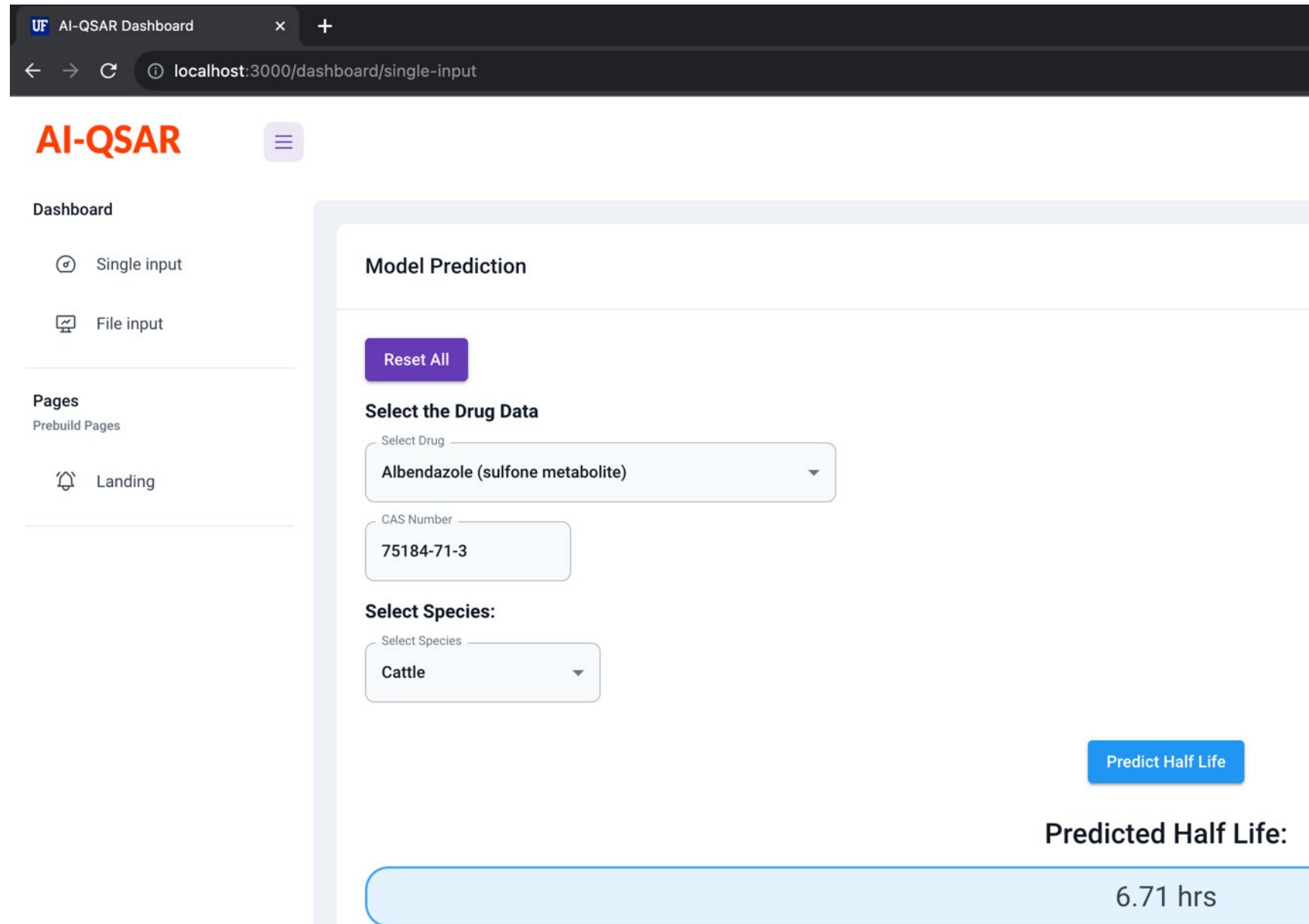
Descriptor	All		RDKit		ECFP		FCFP		MACCS	
	5-fold CV	Test								
Model										
KNN										
R ²	0.21±0.25	0.21	0.09±0.11	0.09	0.15±0.15	0.24	0.16±0.16	0.25	0.01±0.07	0.11
RMSE	35.26±27.47	26.49	36.50±26.28	28.50	35.62±26.09	26.10	35.60±26.27	25.90	37.32±25.39	28.12
RF										
R ²	0.05±0.10	0.12	0.01±0.07	0.12	0.05±0.06	0.12	0.09±0.10	0.17	0.04±0.05	0.20
RMSE	36.36±24.79	28.04	36.77±24.81	28.07	36.84±25.80	28.08	37.02±25.18	27.23	36.93±24.78	26.27
SVM										
R ²	0.25±0.26	0.09	0.23±0.27	0.21	0.33±0.31	0.09	0.34±0.31	0.09	0.35±0.29	0.16
RMSE	34.35±26.82	28.45	34.25±26.25	26.53	32.87±27.14	28.53	32.80±27.07	28.46	32.54±26.85	27.35
DNN										
R ²	0.82±0.19	0.67	0.85±0.21	0.40	0.46±0.31	0.44	0.82±0.24	0.49	0.61±0.23	0.43
RMSE	13.53±8.21	17.23	11.87±10.73	23.24	28.46±13.39	22.30	11.01±8.98	21.31	22.91±8.86	22.66

CV: cross-validation

ECFP: extended-connectivity fingerprints, FCFP: functional-class fingerprints, MACCS: molecular ACCess system

kNN: k-nearest neighbors, RF: random forest, SVM: support vector machine, DNN: deep neural network

Application 1: Preliminary results of the AI-QSAR model



The screenshot shows the AI-QSAR Dashboard interface. The left sidebar includes links for 'Single input' and 'File input'. The main 'Model Prediction' section has a 'Reset All' button. Under 'Select the Drug Data', the 'Select Drug' dropdown is set to 'Albendazole (sulfone metabolite)'. The 'CAS Number' input field contains '75184-71-3'. Under 'Select Species:', the 'Select Species' dropdown is set to 'Cattle'. A blue 'Predict Half Life' button is located to the right of the species selection. Below the button, the text 'Predicted Half Life:' is followed by a light blue bar containing the value '6.71 hrs'.

AI-QSAR

Dashboard

Single input

File input

Pages

Prebuild Pages

Landing

Model Prediction

Reset All

Select the Drug Data

Select Drug: Albendazole (sulfone metabolite)

CAS Number: 75184-71-3

Select Species:

Select Species: Cattle

Predict Half Life

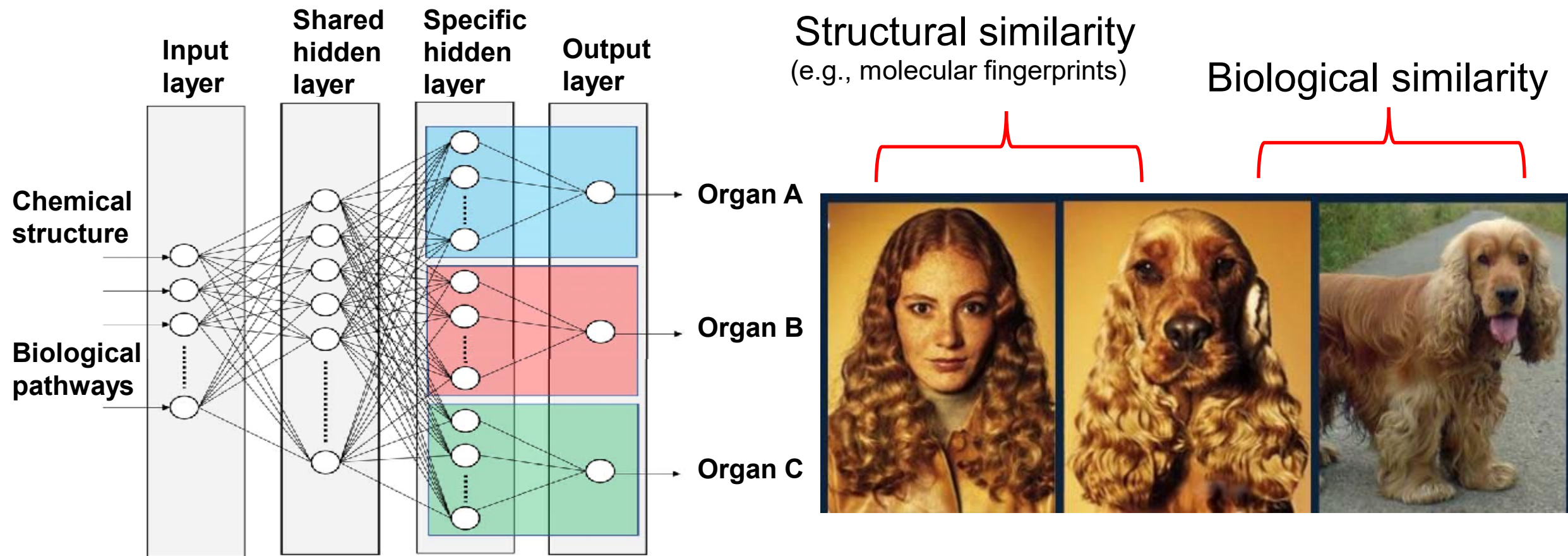
Predicted Half Life:

6.71 hrs

Application 2: AI in Predicting Toxicity

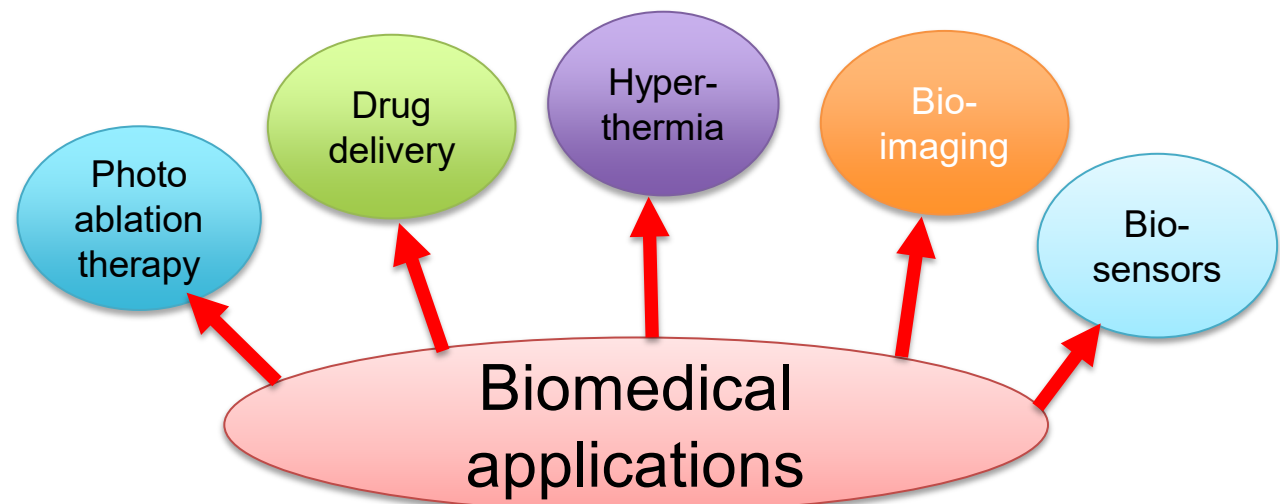
Application 2: AI-based QSAR in predicting toxicity of chemicals

Objective: To develop robust AI-QSAR models to predict human systemic/organ-specific toxicity by using multitask deep learning QSAR modeling approaches

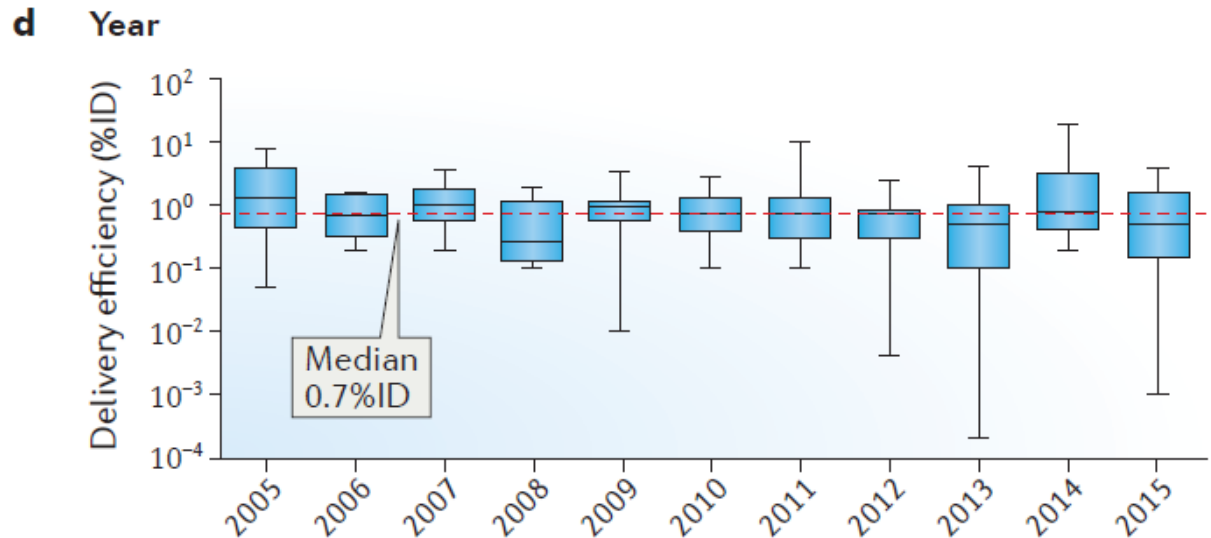


Application 3:
AI-assisted PBPK Model for
Nanoparticle Risk Assessment
Cancer Nanomedicine

Application 3: AI-assisted PBPK model for nanoparticles



Delivery efficiency of NPs to tumors based on studies published each year



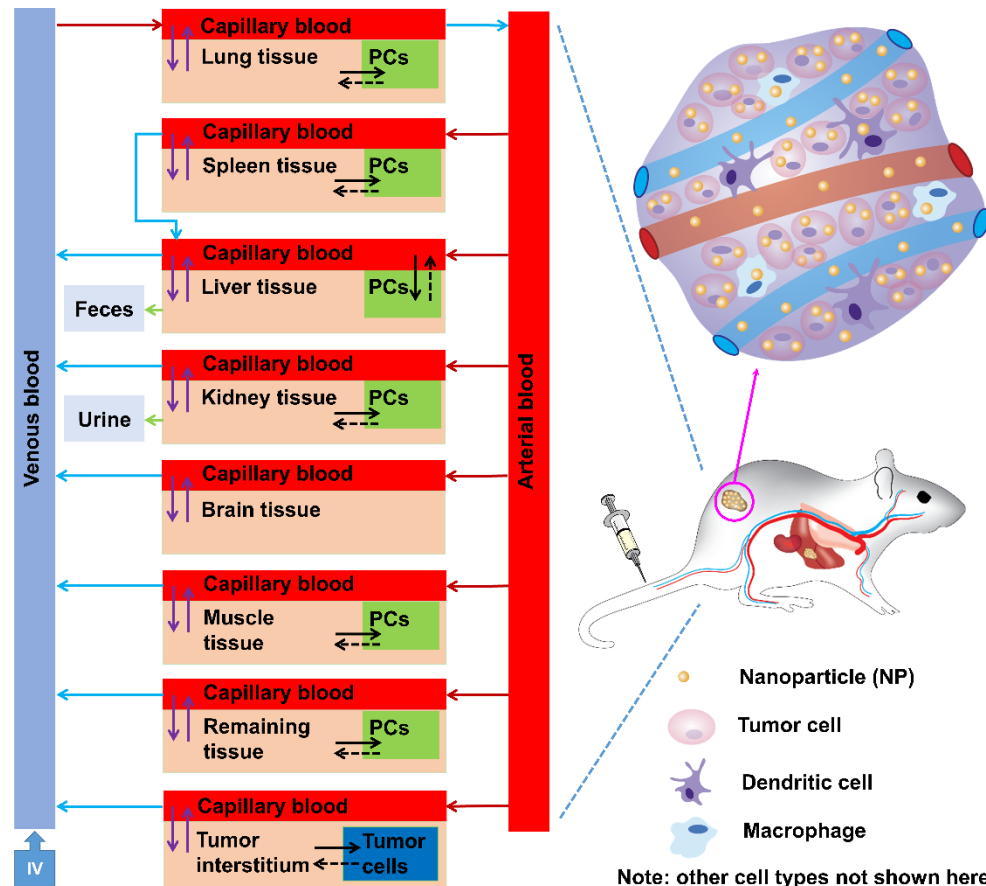
Critical barriers to progress in this field

- Nanotoxicology: lack of robust computational tools to assess risk
- Nanomedicine: low delivery efficiency (<1%) to target tissues (i.e., tumor)

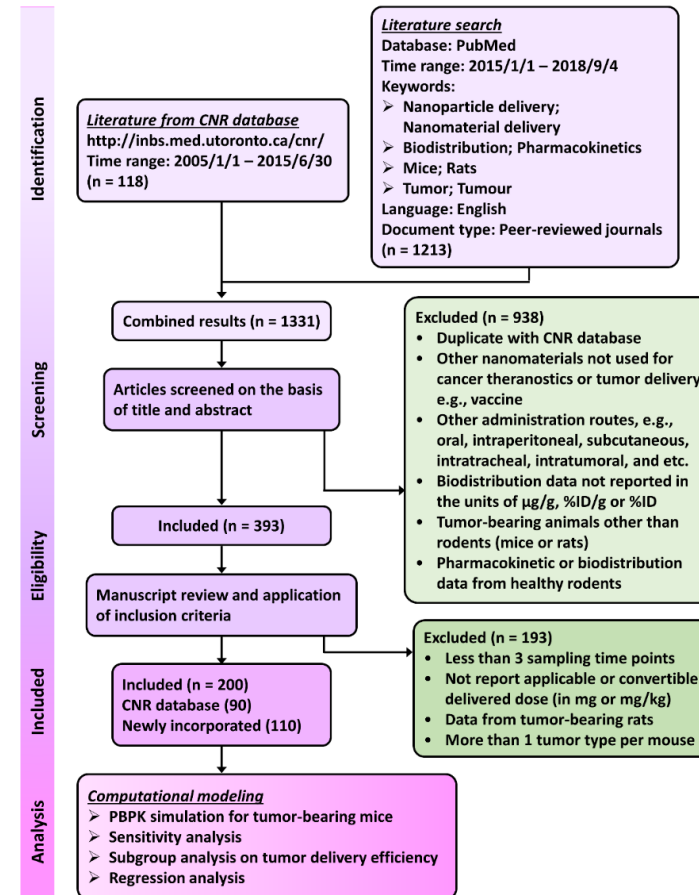
- Wilhelm S, Tavares AJ, Dai Q, Ohta S, Audet J, Dvorak HF, Chan WCW. Analysis of nanoparticle delivery to tumours. 2016. *Nature Reviews Materials*, 1, 16014.
- Cheng YH, He C, Riviere JE, Monteiro-Riviere NA, Lin Z. Meta-Analysis of Nanoparticle Delivery to Tumors Using a Physiologically Based Pharmacokinetic Modeling and Simulation Approach. *ACS Nano*. 2020;14(3):3075-3095. **(Best Paper Award of the Year 2020 – Honorable Mention presented by Society of Toxicology Biological Modeling Specialty Section in 2021)**
- Chen Q, Riviere JE, Lin Z. Toxicokinetics, dose-response, and risk assessment of nanomaterials: Methodology, challenges, and future perspectives. *WIREs Nanomed Nanobiotechnol*. 2022 Nov;14(6):e1808.

Application 3: AI-assisted PBPK model for nanoparticles

PBPK Structure in tumor-bearing mice



Nano-Tumor Database



Note: currently, this database contains 534 datasets from 297 studies published from 2005 to 2021.

Cheng YH, He C, Riviere JE, Monteiro-Riviere NA, Lin Z. (2020). Meta-analysis of nanoparticle delivery to tumors using a physiologically based pharmacokinetic modeling and simulation approach. *ACS Nano*, 14(3): 3075-3095. (Best Paper Award of the Year 2020 – Honorable Mention presented by Society of Toxicology Biological Modeling Specialty Section in 2021)

Chen Q, Yuan L, Chou WC, Cheng YH, He C, Monteiro-Riviere NA, Riviere JE, Lin Z. Meta-Analysis of Nanoparticle Distribution in Tumors and Major Organs in Tumor-Bearing Mice. *ACS Nano*. 2023 Oct 9. doi: 10.1021/acsnano.3c04037. Epub ahead of print. PMID: 37812732.

Application 3: AI-assisted PBPK model for nanoparticles

Our Own “Nano-Tumor Database” for Subsequent Analyses

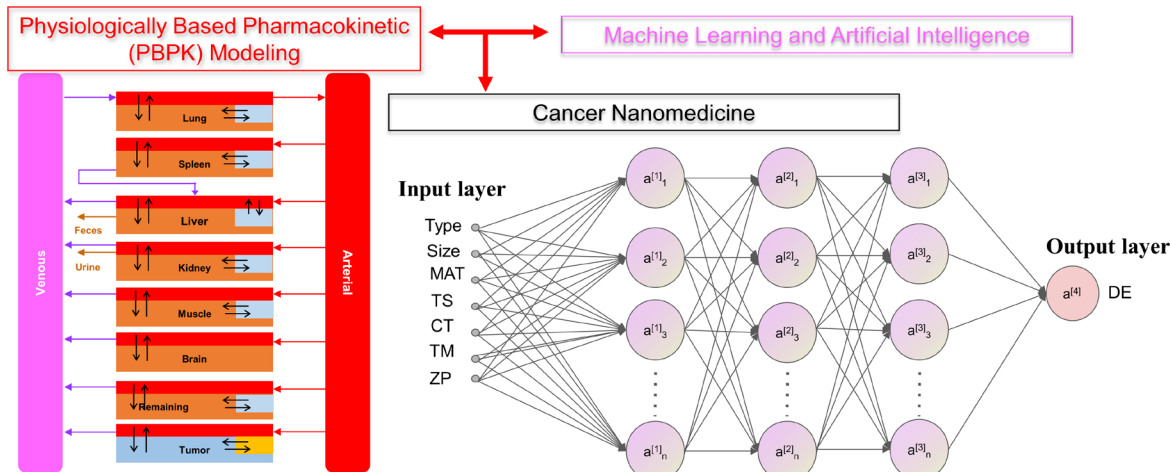
CNR or New Ref. ID	New Ref. No	Type	MAT	TS	CT	TM	Shape	log(HD)	ZP	DE(Tmax)	DE(Tmax)_PK	DE(24)	DE(168)	Max DE	log(DE(Tmax))	log(DE(Tmax)_PK)	log(DE(24))	log(DE(168))	log(Max DE)	Conf. in Predict.
#1 Zhong et al. (2015)	1	Inorganic	Gold	Active	Cervix	XH	Rod	1.38	-18	2.06	1.97	1.69	2.06	2.36	0.31	0.29	0.23	0.31	0.37 Y (R2 = 0.99)	
#3 Goodrich et al. (2010)	2	Inorganic	Gold	Passive	Colon	AH	Rod	1.48	0	1.62	1.51	0.99	0.79	2.39	0.21	0.18	0	-0.1	0.38 Y (R2 = 0.99)	
#4 Meyers et al. (2015)	3	Inorganic	Gold	Passive	Brain	XH	Spherical	1.58	-5	2.99	3.61	6.64	2.99	7.44	0.48	0.56	0.82	0.48	0.87 Y (R2 = 0.87)	
#4 Meyers et al. (2015)	3	Inorganic	Gold	Active	Brain	XH	Spherical	1.62	-5	2.83	2.85	3.27	2.83	4.18	0.45	0.45	0.51	0.45	0.62 Y (R2 = 0.87)	
#5 Dam et al. (2015)	4	Inorganic	Gold	Active	Breast	XH	Other	1.84	-9.3	0.74	0.64	0.42	1.67	1.77	-0.13	-0.19	-0.38	0.22	0.25 Y (R2 = 0.91)	
#6 Sykes et al. (2014)	5	Inorganic	Gold	Active	Skin	XO	Spherical	1.69	-0.6	25.2	25.07	22.86	11	29.88	1.4	1.4	1.36	1.04	1.48 Y (R2 = 0.96)	
#6 Sykes et al. (2014)	5	Inorganic	Gold	Active	Skin	XO	Spherical	1.78	-11	25.83	23.86	26.63	9.94	30.24	1.41	1.38	1.43	1	1.48 Y (R2 = 0.96)	
#6 Sykes et al. (2014)	5	Inorganic	Gold	Active	Skin	XO	Spherical	2	-9	24.4	21.37	26.87	8.77	29.78	1.39	1.33	1.43	0.94	1.47 Y (R2 = 0.96)	
#6 Sykes et al. (2014)	5	Inorganic	Gold	Passive	Skin	XO	Spherical	1.67	-6.7	19.38	18.64	18.11	7.79	23.4	1.29	1.27	1.26	0.89	1.37 Y (R2 = 0.96)	
#6 Sykes et al. (2014)	5	Inorganic	Gold	Passive	Skin	XO	Spherical	1.81	-15	14.63	14.28	14.71	5.47	17.52	1.17	1.15	1.17	0.74	1.24 Y (R2 = 0.96)	
#6 Sykes et al. (2014)	5	Inorganic	Gold	Passive	Skin	XO	Spherical	2.02	-10	12.17	11.19	11.98	4.53	14.77	1.09	1.05	1.08	0.66	1.17 Y (R2 = 0.96)	
#6 Sykes et al. (2014)	5	Inorganic	Gold	Active	Skin	XO	Spherical	2.24	-5	8.79	8.21	9.61	2.98	11.15	0.94	0.91	0.98	0.47	1.05 Y (R2 = 0.96)	
#6 Sykes et al. (2014)	5	Inorganic	Gold	Passive	Skin	XO	Spherical	2.22	-6	5.18	4.94	5.63	4.25	6.41	0.71	0.69	0.75	0.63	0.81 Y (R2 = 0.96)	
#7 Hu et al. (2014)	6	Inorganic	Gold	Passive	Brain	XH	Spherical	0.79		1.13	1.12	1.13	0.37	1.34	0.05	0.05	0.05	-0.43	0.13 Y (R2 = 0.98)	
#8 Razzak et al. (2013)	7	Inorganic	Gold	Passive	Prostate	XH	Spherical	1.44		0.13	0.06	0.11	0.03	0.14	-0.89	-1.22	-0.96	-1.52	-0.85 N (R2 = 0.67)	
#9 Liu et al. (2014)	8	Inorganic	Gold	Passive	Cervix	XH	Spherical	1.23	-9.8	1.24	1.13	1.02	0.76	1.55	0.09	0.05	0.01	-0.12	0.19 Y (R2 = 0.94)	
#9 Liu et al. (2014)	8	Inorganic	Gold	Passive	Cervix	XH	Spherical	1.49	-10.5	0.64	0.54	0.7	0.32	0.86	-0.19	-0.27	-0.15	-0.49	-0.07 Y (R2 = 0.94)	
#10 Cheng et al. (2014)	9	Inorganic	Gold	Active	Brain	XH	Other	1.38	-21.3	1.63	1.57	1.58	0.65	1.87	0.21	0.2	0.2	-0.19	0.27 Y (R2 = 0.97)	
#10 Cheng et al. (2014)	9	Inorganic	Gold	Passive	Brain	XH	Other	1.41	21.7	0.61	0.59	0.57	0.26	0.69	-0.21	-0.23	-0.24	-0.59	-0.16 Y (R2 = 0.97)	
#10 Cheng et al. (2014)	9	Inorganic	Gold	Passive	Brain	XH	Other	1.32	24.6	0.55	0.51	0.54	0.22	0.61	-0.26	-0.29	-0.27	-0.66	-0.21 Y (R2 = 0.97)	
#10 Cheng et al. (2014)	9	Inorganic	Gold	Passive	Brain	XH	Other	1.26	25.4	0.38	0.36	0.4	0.15	0.43	-0.42	-0.44	-0.4	-0.82	-0.37 Y (R2 = 0.97)	
#11 Zhang et al. (2015)	10	Inorganic	Gold	Active	Stomach	XH	Spherical	0.79	-5	9.1	9.52	10.68	9.1	12.46	0.96	0.98	1.03	0.96	1.1 Y (R2 = 0.82)	
#12 Black et al. (2014)	11	Inorganic	Gold	Passive	Breast	AH	Spherical	1.84	0	4.02	1.74	4.02	2.11	6.09	0.6	0.24	0.6	0.32	0.78 Y (R2 = 0.99)	
#12 Black et al. (2014)	11	Inorganic	Gold	Passive	Breast	AH	Other	2.05	0	1.65	0.62	1.65	0.55	2.14	0.22	-0.21	0.22	-0.26	0.33 Y (R2 = 0.99)	
#12 Black et al. (2014)	11	Inorganic	Gold	Passive	Breast	AH	Plate	2.12	0	1.23	0.46	1.23	0.37	1.46	0.09	-0.34	0.09	-0.43	0.16 Y (R2 = 0.99)	
#12 Black et al. (2014)	11	Inorganic	Gold	Passive	Breast	AH	Rod	1.89	0	0.47	0.15	0.47	0.17	0.61	-0.33	-0.82	-0.33	-0.77	-0.21 Y (R2 = 0.99)	
#13 Liu et al. (2013)	12	Inorganic	Gold	Passive	Breast	XO	Spherical	0.74	0	1.26	1.24	1.54	0.41	1.74	0.1	0.09	0.19	-0.39	0.24 Y (R2 = 0.70)	
#14 Karmani et al. (2013)	13	Inorganic	Gold	Active	Skin	XO	Spherical	1.49		2.25	2.23	1.53	2.25	2.52	0.35	0.35	0.18	0.35	0.4 Y (R2 = 0.97)	
#15 Wang et al. (2012)	14	Inorganic	Gold	Passive	Breast	AH	Other	1.8	10.2	2.67	2.45	2.67	0.8	3.07	0.43	0.39	0.43	-0.1	0.49 Y (R2 = 0.99)	
#15 Wang et al. (2012)	14	Inorganic	Gold	Passive	Breast	AH	Other	1.98	18.7	0.48	0.44	0.48	0.14	0.52	-0.32	-0.36	-0.32	-0.85	-0.28 Y (R2 = 0.99)	
#16 Shah et al. (2012)	15	Inorganic	Gold	Passive	Prostate	XH	Spherical	1.82	-2.6	0.67	0.64	0.67	0.21	0.79	-0.17	-0.19	-0.17	-0.68	-0.1 Y (R2 = 0.99)	
#16 Shah et al. (2012)	15	Inorganic	Gold	Passive	Prostate	XH	Spherical	1.8	-27.1	0.6	0.59	0.6	0.17	0.71	-0.22	-0.23	-0.22	-0.77	-0.15 Y (R2 = 0.99)	
#16 Shah et al. (2012)	15	Inorganic	Gold	Active	Prostate	XH	Spherical	1.86	-2.9	0.61	0.55	0.61	0.21	0.85	-0.21	-0.26	-0.21	-0.68	-0.07 Y (R2 = 0.99)	

Note: By 2020, this database contains 376 datasets from 200 studies published from 2005 to 2018. By 2023, this database contains 535 datasets from 298 studies published from 2005 to 2021.

- Cheng YH, He C, Riviere JE, Monteiro-Riviere NA, Lin Z*. (2020). Meta-analysis of nanoparticle delivery to tumors using a physiologically based pharmacokinetic modeling and simulation approach. *ACS Nano*, 14(3): 3075-3095. (**Best Paper Award of the Year 2020 – Honorable Mention presented by Society of Toxicology Biological Modeling Specialty Section in 2021**)
- Chen Q, Yuan L, Chou WC, Cheng YH, He C, Monteiro-Riviere NA, Riviere JE, Lin Z*. (2023). Meta-Analysis of Nanoparticle Distribution in Tumors and Major Organs in Tumor-Bearing Mice. *ACS Nano*, in press.

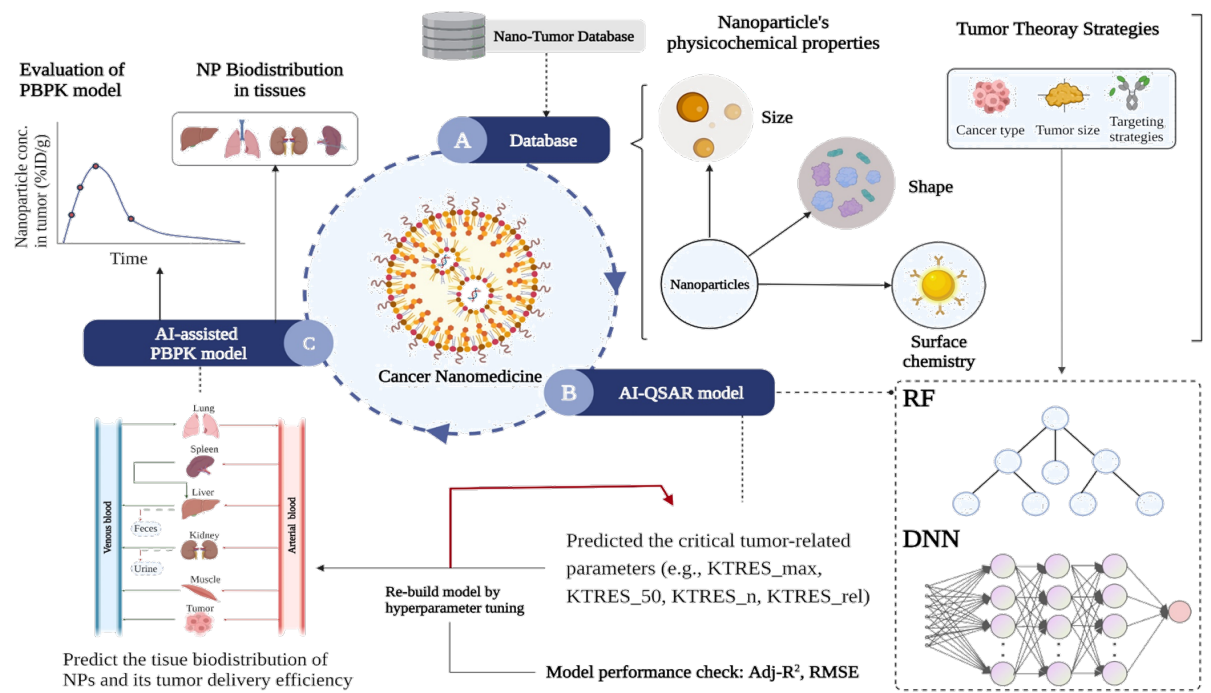
Application 3: Integration of AI with PBPK to predict tumor delivery efficiency

A data-driven approach



Lin Z, Chou WC, Cheng YH, He C, Monteiro-Riviere NA, Riviere JE. (2022). Predicting Nanoparticle Delivery to Tumors Using Machine Learning and Artificial Intelligence Approaches. *International Journal of Nanomedicine*, 17:1365-1379.

A hybrid approach



Chou WC, Chen Q, Cheng YH, He C, Monteiro-Riviere NA, Riviere JE, Lin Z. (2023). An artificial intelligence-assisted physiologically-based pharmacokinetic model to predict nanoparticle delivery to tumors in mice. *Journal of Controlled Release*, 361:53-63..

Summary and Discussion

- By leveraging machine learning and artificial intelligence approaches, now it is possible to:
 - (1) AI-QSAR models to predict ADME properties of hundreds of chemicals
 - (2) AI-PBPK models for hundreds of chemicals
 - (3) AI-QSAR models to predict toxicity for a large number of chemicals
 - (4) Analyze a large amount of different types of data to generate new insights into toxicity mechanisms rapidly, which was difficult by manual approaches in the past.
- Several challenges should be considered:
 - (1) Evaluate different methods to determine the optimal approach
 - (2) Bioactivity classification (yes/no) vs. the intensity of effect or dose-response relationship
 - (3) Rigorous data quality check and infrastructure to store, share, analyze, evaluate, and manage big data
 - (4) User-friendly interfaces to facilitate applications of AI-QSAR/PBPK models



ChatGPT is smart enough to pass the MBA and USMLE tests... Is DABT next?

2023 Toxicology Forum Summer Meeting

Acknowledgements

Lab members:

Zhoumeng Lin
Wei-Chun Chou
Qiran Chen
Xue Wu
Kun Mi
Malek Hussein Hajjawi
Pei-Yu Wu
Chi-Yun Chen
Venkata Nithin Kamineni
Yashas Kuchimanchi
Zhicheng Zhang
Ethan Cecil



UGA 2013

Former members: Collaborators: Advisors:

Miao Li
Yi-Hsien Cheng
Long Yuan
Md Mahbubul Huq Riad
Dongping Zeng
Trevor Elwell-Cuddy
Paula Solar; Sichao Mao
Yilei Zheng; Yi-Jun Lin
Ning Xu; Yu Shin Wang
Jake Willson
Gabriel (Guanyu) Tao

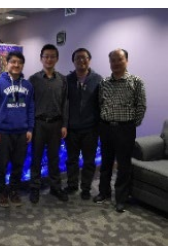


KSU 2017

Collaborators: Advisors:

ICCM/NICKS/KSU
EGH/CEHT/UF
CPSP/UF
FARAD Team

Dr. Jim E. Riviere
Dr. Nancy A. Monteiro-Riviere
Dr. Nikolay M. Filipov
Dr. Jeffrey W. Fisher
Dr. Ronette Gehring



KSU Lab 2019

Active Funding:

- NIH/NIBIB Grant #: R01EB031022
- USDA/NIFA Award #: 2023-41480-41035
- USDA/NIFA Award #: 2022-41480-38137
- USDA/NIFA Award #: 2021-41480-35271
- USDA/NIFA Award #: 2021-67015-34084
- UF PHHP PhD Fellowship in Artificial Intelligence

Completed Funding:

- USDA/NIFA Award #: 2020-41480-32497
- USDA/NIFA Award #: 2020-67015-31456
- USDA/NIFA Award #: 2020-67030-31479
- CHOP subaward #: FP37698_SUB01_01
- NIH/NIBIB Grant #: R03EB026045
- USDA/NIFA Award #: 2019-41480-30296
- USDA/NIFA Subaward #: A20-2028-S002
- NIH/NIBIB Grant #: R03EB025566
- USDA/NIFA Award #: 2018-41480-28805
- USDA/NIFA Award #: 2017-68003-26499
- USDA/NIFA Award #: 2017-41480-27310
- USDA/NIFA Award #: 2016-41480-25729
- AASV Foundation Grant Award #: A00-1103-001
- K-State CVM SUCCESS-FYI Program
- K-State Mark Derrick Canine Research Fund
- K-State Global Campus Internal Grant Program
- K-State Mentoring Fellowship
- K-State University Small Research Grant (USRG)

Food Animal Residue Avoidance Databank

(A component of the Food Animal Residue Avoidance & Depletion Program)



NIBIB

National FARAD 2019



UF FARAD 2021 National FARAD 2022